SECOND EUROPEAN CONFERENCE ON EARTHQUAKE ENGINEERING
AND SEISMOLOGY, ISTANBUL AUG. 25-29, 2014

NONLINEAR FINITE ELEMENT MODELING OF REINFORCED CONCRETE STRUCTURAL WALLS

Muhammet Fethi GULLU[1] and Kutay ORAKCAL[2]

ABSTRACT

This paper presents a new finite element modeling approach to predict the nonlinear inelastic response of reinforced concrete (RC) structural walls under generalized reversed-cyclic, in-plane loading conditions. An important motivation of this study is related to simulation of nonlinear shear behavior of structural walls, as well as the interaction between nonlinear flexural and shear responses. The proposed finite element model incorporates constitutive RC panel elements, the behavior of which is represented by a fixed crack angle modeling approach. The model formulation was implemented into Matlab, analyses were performed using a drift-controlled nonlinear analysis solution strategy, and model predictions were compared with test results obtained for a heavily-instrumented and relatively slender wall specimen. The model demonstrated a reasonable level accuracy in predicting the nonlinear hysteretic response of the wall investigated. Accurate predictions were obtained for the experimentally-observed cyclic response characteristics of the wall, including its lateral load capacity, stiffness degradation, hysteretic shape, plastic (residual) displacements, ductility, and pinching behavior. The model also provided reasonably accurate predictions of nonlinear flexural deformations developing in the plastic hinge region of the wall. Average longitudinal strain profiles along the base of the wall were reasonably predicted by the model. The analytical model also provided reasonable estimates for the nonlinear shear deformations developing along the first story height of the wall, where nonlinear flexural deformations were also concentrated. The magnitude of the predicted nonlinear shear deformations decreased along the wall height, which was consistent with the experimental measurements. This demonstrated the model's capability of capturing nonlinear shear-flexure interaction effects in a relatively slender wall.

INTRODUCTION

Reinforced concrete (RC) structural walls are commonly used because of their significant contribution to resistance against lateral actions imposed on building structures, including earthquake effects and wind loads. Presence of structural walls has considerable impact on strength and stiffness characteristics, as well as the deformation capacity of structures. The effectiveness of structural walls makes it important to understand and characterize their hysteretic behavior when subjected to earthquake actions. Therefore, numerous analytical and experimental studies have been conducted on investigating the lateral load behavior of RC walls. Experimental and analytical studies are essential for nonlinear response prediction of walls, both within the context of performance-based assessment procedures, and for improvement of design provisions.

There are various computer programs for the analysis of structural systems, almost all of which incorporate significant defects due to not representing important behavioral characteristics associated

[1] Res. Assist., Bogazici University, Istanbul, fethi.gullu@boun.edu.tr
[2] Assoc. Prof., Bogazici University, Istanbul, kutay.orakcal@boun.edu.tr

with the nonlinear hysteretic behavior of RC structural walls. With implementation of the performance-based analysis and design approaches in modern seismic codes, detailed modeling of the nonlinear behavior of walls has gained much importance. While representing the linear elastic behavior of walls is not a significant challenge in design, there is still a considerable need for reliable analytical modeling approaches for robust simulation of the nonlinear hysteretic behavior of walls. In theory, analytical modeling of the inelastic response of RC walls can be conducted by using either microscopic (e.g., finite element) or macroscopic (e.g., plastic hinge or fiber) modeling approaches. Microscopic modeling approaches are typically not used in performance-based design applications, due to complexities in their implementation and calibration, as well as interpretation of the results. A widely-known and commonly-used finite element modeling approach for nonlinear analysis and design of structural walls is still not available. On the other hand, macroscopic modeling approaches available in the literature, with the so-called fiber models being the most common, are generally sufficient for modeling of uncoupled shear and flexural responses in a wall. The well known Multiple-Vertical-Line Element Model (MVLEM) was first proposed by Vulcano *et al.* (1988) as an efficient fiber-based modeling approach for simulating the nonlinear flexural behavior of RC structural walls. Due to complexities in modeling of material behavior, additional studies were conducted by Fischinger *et al.* (1990) to simplify the constitutive models implemented in the MVLEM without impairing the accuracy of the results. A more recent study was conducted by Orakcal *et al.* (2004) in order to establish more robust constitutive material models in formulation of the MVLEM. However, such fiber-based macroscopic modeling approaches have been shown to be unsuccessful in capturing the nonlinear shear and shear-flexure interaction behavior, which have been observed experimentally for even slender walls. Although consideration of nonlinear shear behavior is typically deemed important for response prediction of squat (low-rise) walls; unexpected shear yielding behavior, nonlinear shear deformations, and nonlinear shear-flexure interaction effects have also been observed experimentally for slender walls that have been designed to yield in flexure and are expected to show linear elastic shear behavior. Hence, there is still a need for robust modeling methodologies, using meso-scale approaches, which can capture such behavioral attributes in RC structural walls.

Given these shortcomings, in this study, a relatively simple yet robust finite element model formulation is developed for simulating the in-plane behavior of RC structural walls under reversed cyclic loading conditions; one which considers nonlinear flexural and shear responses, as well as their interaction throughout the loading history. A recent constitutive model for RC panels, named the Fixed Strut Angle Model (FSAM), proposed for simulating the cyclic shear behavior of reinforced concrete panel elements (Ulugtekin, 2010, Orakcal *et al.,* 2012) is adopted in the two-dimensional finite-element model formulation, due to its accuracy and relatively simple formulation. The finite element model formulation with the constitutive Fixed Strut Angle panel model is implemented in Matlab, together with a nonlinear analysis solution strategy. The model is calibrated and validated against experimental results obtained for a relatively slender RC wall specimen tested previously. Model response predictions are evaluated for assessment of the capabilities of the model, as well as for identifying potential model improvements.

ANALYTICAL MODEL

A rectangular two-dimensional finite element modeling approach was adopted for modeling of RC structural walls. The constitutive membrane (panel) elements incorporate two degree of freedoms (DOFs) at each node, in vertical and horizontal directions, and do not incorporate any rotational DOFs. Formulation of the constitutive membrane elements are valid for in-plane conditions only, implying that only in-plane stiffness is considered and only in-plane loads are admissible. Description of the nonlinear behavior of the membrane elements requires a constitutive RC panel element formulation for representing the constitutive behavioral features of reinforced concrete including hysteretic material behavior, compression softening, tension stiffening, hysteretic biaxial damage, and shear transfer across cracks. The constitutive panel model selected for implementation into the two dimensional finite element model is the Fixed Strut Angle Model (FSAM) proposed by Ulugtekin (2010).

In the constitutive panel model implemented, as it is typically assumed in other RC panel elements available in the literature, assumptions of perfect bond between concrete and reinforcing steel and no dowel action on reinforcing bars are used. Dowel action effects (shear stresses perpendicular to the longitudinal direction of the reinforcing steel) are typically deemed negligible in the nonlinear shear behavior of RC members, especially under high levels of shear strain. For the hysteretic constitutive modeling of reinforcing steel bars, uniaxial directions along the rebar directions are used, whereas for the constitutive modeling of concrete stress-strain behavior, biaxial relations along the fixed strut (crack) directions are incorporated.

A rotating strut approach, similar to the Modified Compression Field Theory (Vecchio and Collins, 1986) and the Rotating Angle Strut and Tie Model (Pang and Hsu, 1995) are used for simulation of the biaxial stress-strain behavior of uncracked concrete. For the uncracked loading stages of the RC panel, the hysteretic behavior of concrete was assumed to be monotonic, which is for small strains prior to cracking. At this stage, the principal strain directions obtained from the applied strain field were assumed to coincide with principal stress directions in concrete. The constitutive material model for concrete is therefore applied along the principal strain directions (Figure 1(a).).

When the principal tensile strain first exceeds the monotonic cracking strain value of concrete, the first crack forms in the RC panel model, in perpendicular direction to the principal tensile strain. Formation of the first crack means that for subsequent loading, the first "Fixed Strut" direction, which is parallel to the first crack, is assigned. For further stages of loading, principal stress directions in concrete coincide with the first crack directions (parallel and perpendicular), while principal strain directions continue to rotate with the applied strain field. Since the first crack direction coincides with principal stress directions in concrete, zero shear stress (zero shear aggregate interlock) develops along the crack, which is an inherent assumption in the original FSAM formulation. After formation of the first crack, the hysteretic stress-strain relationship for concrete is used in directions parallel and perpendicular to the fixed strut. Calculation of these principal stresses in concrete is only possible with transformation of the strain field into directions parallel or perpendicular to the fixed strut, rather than the principal strain directions. After calculation of the strains parallel and perpendicular to the fixed strut direction, concrete stress values are determined by using the uniaxial constitutive model adopted for concrete. Calculated stresses in parallel and perpendicular directions to the fixed strut are reduced by biaxial compression softening and biaxial damage parameters. The hysteretic uniaxial constitutive material model implemented for reinforcing steel is applied along the orthogonal rebar directions to calculate the stresses in reinforcing steel. Superposition of stresses developing in concrete and reinforcing steel (using reinforcing steel area ratios) provides the resultant averages stresses on the panel element. Behavior of concrete in the FSAM after formation of the first crack is illustrated in Figure 1(b).

Until the formation of the second crack, the constitutive behavior proceeds in the form of a single fixed strut mechanism. When the tensile strain along the first strut direction exceeds the cracking strain of concrete, the second crack is formed. The second crack is formed perpendicular to the first crack because of the zero shear stress assumption along the crack directions. The first and second cracks in the panel element are therefore orthogonal. Examples of this “orthogonal crack” modeling approach are common in the literature. Formation of the second crack perpendicular to the first fixed strut implies formation of the second "fixed strut". Depending on the loading direction, these fixed struts work under tension or compression. For subsequent loading stages, principal stress directions in concrete are fixed along the fixed strut directions, whereas principal strain values are free to rotate. In order to determine the principal stresses in concrete, the applied strain field is transformed into strain components in the fixed strut directions instead of principal strain directions. Calculated strain values parallel to the two fixed strut directions are used in the uniaxial constitutive model for concrete to obtain the principal stresses in concrete, and the concrete stresses are reduced by compression softening and biaxial damage parameters. Again, the constitutive material model for reinforcing steel is applied along the orthogonal rebar directions and superposition of stresses developing in concrete and reinforcing steel gives the resultant averages stresses on the panel element. Behavior of concrete in the FSAM after formation of the second crack is shown in Figure 1(c).

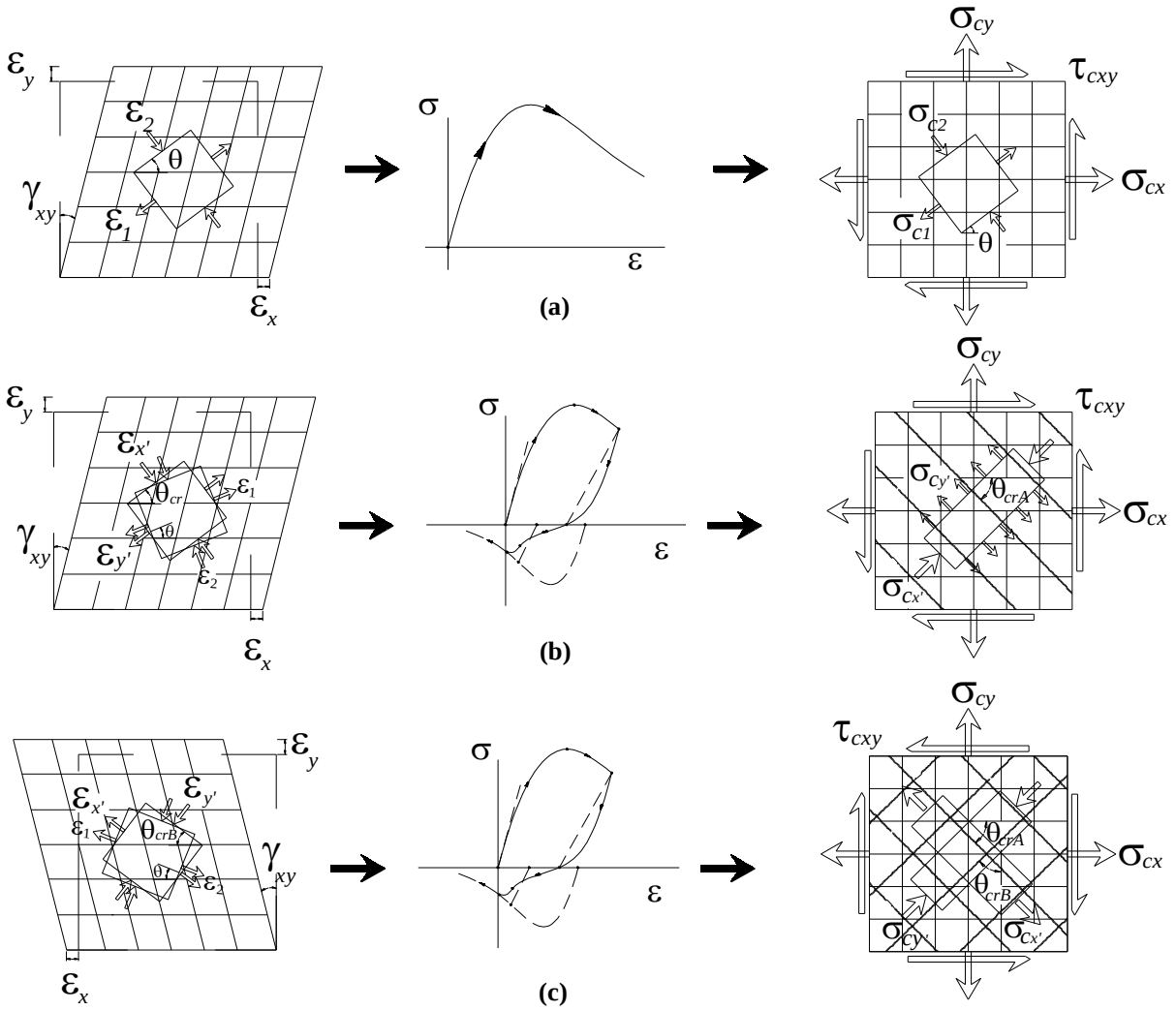

Figure 1. Concrete biaxial behavior in the Fixed Strut Angle Model: (a) uncracked behavior, (b) behavior after formation of first crack, (c) behavior after formation of second crack (Orakcal *et al.*, 2012).

Robust material constitutive relationships were adopted in the finite element model formulation to represent the hysteretic stress-strain behavior of concrete and reinforcing steel. The implemented stress-strain behavior for concrete is the uniaxial hysteretic constitutive model proposed by Chang and Mander (1994) (Figure 2(a)). The Chang and Mander model has been shown to provide accurate representation of the experimental results presented by various researchers. Mander *et al.* (1988) calibrated the model for unconfined and confined concrete in cyclic compression. Experimental validation studies against test results reported by Gopalaratnman and Shah (1985) and Yankelevsky and Reinhardt (1987) have shown that the model provides reliable results for unconfined and confined concrete under cyclic tension and compression. The implemented constitutive hysteretic material model for reinforcing steel is the well-known nonlinear hysteretic relationship of Menegotto and Pinto (1973), extended by Filippou *et al.* (1983) to represent isotropic strain hardening. This constitutive model, although simple in formulation, has been shown to accurately represent experimental results on reinforcing steel bars. The constitutive model represents the so-called Bauschinger's effect, by including cyclic degradation of stiffness along the unloading and reloading curves. A description of the constitutive model is depicted in Figure 2(b). This constitutive model implemented for concrete was modified by adding compression softening (defined by Vechio and Collins, 1993), hysteretic biaxial damage (defined by Mansour *et al.*, 2002) and tension stiffening effects (defined by Belarbi and Hsu, 1994) into the formulation. These modifications to the constitutive model allow simulating the behavioral features of concrete under biaxial loading conditions. Detailed information on these behavioural features and constitutive parameters are provided in the thesis by Ulugtekin (2010).

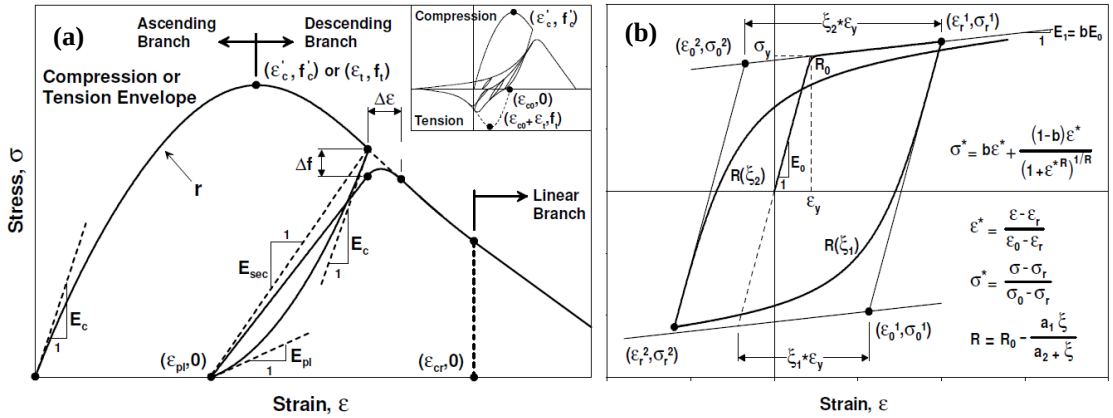

Figure 2. Constitutive material models: (a) concrete (b) reinforcing steel (Orakcal *et al.*, 2012).

The original formulation of the Fixed Strut Angle constitutive panel model described in this paperwas developed by Ulugtekin (2010). However, shear aggregate interlock effects were neglected in the original formulation. Orakcal *et al.* (2012) implemented a simple friction-based elasto-plastic shear aggregate interlock model into the panel model formulation. In this study, the main modification to the constitutive panel model is incorporation of the contribution of reinforcing steel in the shear aggregate interlock mechanism. The yield capacity of the friction-based aggregate interlock model was modified based on ACI 318-11 provisions (Figure 3(a)), for considering the influence of reinforcing steel in the shear-friction capacity.

The cyclic shear aggregate interlock relationship incorporated in the model starts with linear loading/unloading behavior, relating the sliding shear strain along a crack to the shear stress, via a simple linear elastic relationship between the sliding shear strain and the resultant shear stress along the crack surface. When the contribution of reinforcing steel to the shear stress is not considered, the shear stress is restrained to zero value when the concrete normal stress perpendicular to the crack is tensile (crack open); and is bounded via the product of a friction coefficient (η) and the concrete normal stress perpendicular to the crack (Figure 3(b)), when the concrete normal stress is compressive (crack closed). When the contribution of reinforcing steel on the aggregate interlock capacity is also considered, as was done in this study, the interlock shear capacity (V_n) along a crack is calculated using Equation 1 when the reinforcement is perpendicular to the crack, and Equation 2 when the reinforcement is inclined with respect to the crack:

$$V_n = \eta\,(A_{vf}\,f_y + N) \tag{1}$$

$$V_n = \eta\,(A_{vf}\,f_y \sin\alpha + N) \tag{2}$$

where η is the friction coefficient, $A_{vf}f_y$ is the axial force corresponding to tensile yielding in reinforcing steel due to sliding shear along the crack surface, N is the normal compressive force in concrete perpendicular to the crack, and α is the angle between the reinforcement and the crack plane (Figure 3(a)).

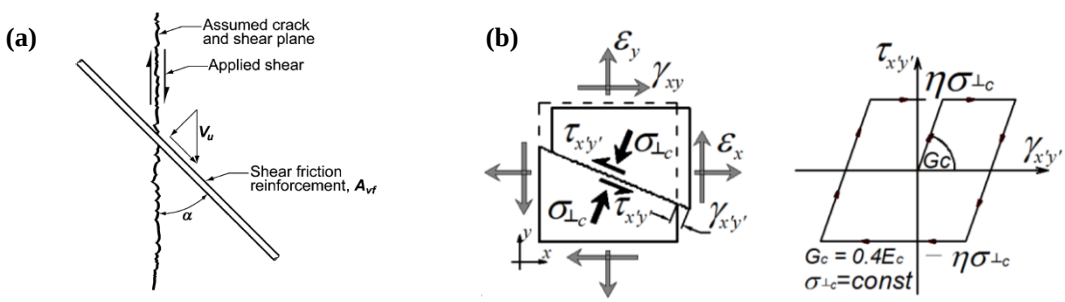

Figure 3. (a) Shear-friction mechanism along a crack (ACI-318M, 2011), (b) Friction-based constitutive model used to represent aggregate interlock behavior (Orakcal et al., 2012).

The linear unloading/reloading slope of the shear stress vs. sliding strain relationship was taken as a fraction of the concrete elastic modulus (a value $0.4E_c$ was adopted, representing the elastic shear modulus of concrete), and a value of 1.0 was assumed for the friction coefficient. Under constant compressive stress in concrete perpendicular to the crack, this model yields an elasto–plastic aggregate interlock behavior under cyclic loading, similar to the cyclic stress–strain behavior of reinforcing steel (Figure 3(b)).

EXPERIMENTAL CALIBRATION AND VALIDATION OF THE MODEL

The analytical model was calibrated to represent the geometric properties, reinforcement configuration, and material characteristics of heavily-instrumented wall specimen RW2 (Figure 4) tested by Thomsen and Wallace (1995, 2003). Calibration of the analytical model consisted of two stages: calibration of the model geometry and calibration of the constitutive material model parameters. As shown in Figure 4(b), in the model formulation, the wall specimen was discretized using 6 segments (m=6) in horizontal direction, and 36 segments (n=36) in the vertical direction, resulting in a total of 216 rectangular model elements. The criteria for model discretization was to make the model elements have approximately equal width and height, and capture the locations where displacement sensors were attached for measurement of local deformations, so that model results can be compared with test measurements also at local response levels.

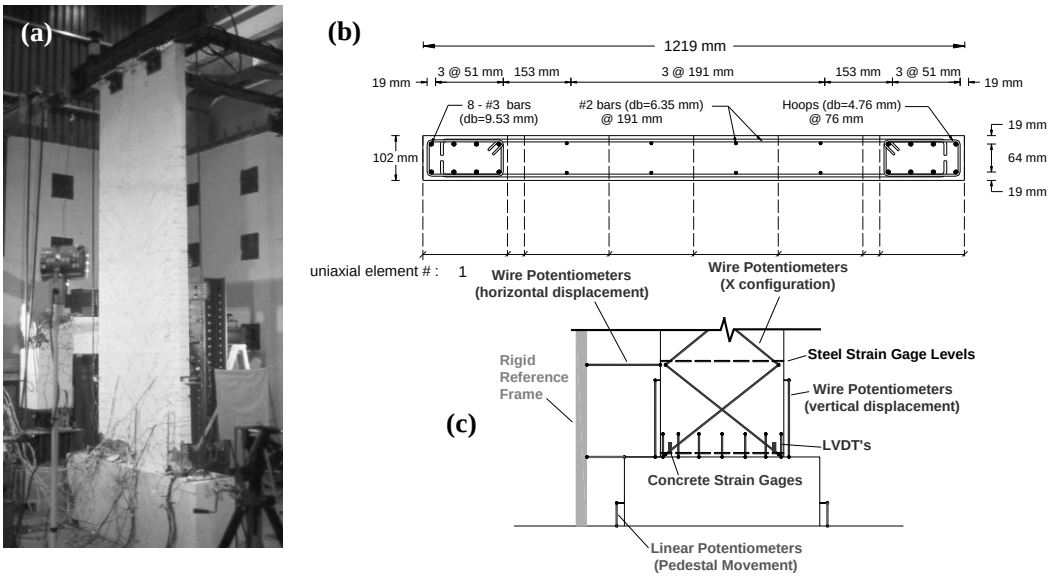

Figure 0. Wall Specimen RW2 (Thomsen and Wallace, 2003): (a) Test Setup, (b) Discretization of the Cross-Section, (c) Instrumentation in the Plastic Hinge Region

Calibration of the model for material properties was performed by calibrating the constitutive model parameters for concrete and reinforcing steel. For the reinforcing steel stress-strain relationship, the monotonic envelope of the Menegotto and Pinto (1977) model was calibrated to represent experimentally-observed results for the reinforcing bars. Based on the test results conducted on bare coupon samples of #3 (d_b = 9.5 mm) and #2 (d_b = 6.3 mm) deformed bars, a modulus of elasticity E_c = 200 GPa, tensile yield strengths of σ_y = 434 MPa and σ_y = 448 MPa, and a strain-hardening ratio of b = 0.02 were assigned the #3 and #2 bars, respectively. These parameters were used to define the monotonic stress-strain envelope of the bars under compression. However, for tension, the yield strength (σ_y) and strain-hardening (b) parameters were modified to include the effects of tension stiffening based on the empirical relation proposed by Belarbi and Hsu (1994). For the calibration of cyclic Bauschinger's effect parameters in the constitutive model for reinforcing steel, namely parameters, R_0, a_1, and a_2, values of $R_0 = 20$, $a_1 = 18.5$, $a_2 = 0.0015$ were assigned to the parameters, as recommended previously by Elmorsi *et al.* (1998).

The Chang and Mander (1994) model was calibrated to represent the experimentally-measured behavior of concrete cylinder samples. An unconfined concrete compressive strength of $f_c' = 42.8$ MPa was assigned, at the compressive strain value of $\varepsilon_c' = 0.0021$. The initial tangent modulus (elastic modulus) of concrete was assigned a value of $E_c = 31026$ MPa. In the compression zone, parameter *r*, which is used for determining the shape of envelope curve, is assigned a value equal to 7.0. Concrete tensile strength f_t was calculated as 2.03 MPa, and the tensile strain value at peak monotonic tensile stress was set equal to $\varepsilon_t = 0.00008$, based on recommendations of Belarbi and Hsu (1994). The initial tangent modulus of concrete in tension was selected to be the same as in compression, which was $E_c = 31026$ MPa, based on the concrete cylinder test results. Unlike the compression envelope, the *r* value for tension was set equal to 1.2, to represent the effects of tension stiffening in the shape of tension envelope curve, as proposed by Belarbi and Hsu (1994). Confined concrete in the boundary regions was calibrated based on the confinement model by Mander *et al.* (1988). In order to achieve consistency in representation of the confinement effect, results obtained using the the model by Mander *et al.* (1998) were compared with the confinement model by Saatcioglu and Razvi (1992). An overall summary of the calibrated constitutive material parameters is presented in Table 1 and Table 2 for concrete and reinforcing steel bars, respectively. Details on calibration of the model parameters are provided in the thesis by Gullu (2013).

Table 1. Calibrated constitutive parameters for concrete.

Concrete in Compression		
Parameter	Boundary (Confined)	Web (Unconfined)
f_c' (Mpa)	47.6	42.8
E_c (Mpa)	31026	31026
ε_c'	0.0033	0.0021
ε_{cr}	0.0037	0.0022
r	1.90	7.00

Concrete in Tension	
Parameter	Boundary & Web (Confined & Unconfined)
f_t (Mpa)	2.03
E_t (Mpa)	31026
ε_t	0.00008
ε_{cr}	∞
r	1.20

Table 2. Calibrated constitutive parameters for reinforcing steel.

Rebar in Compression		
Parameter	#3 Rebar	#2 Rebar
σ_y (Mpa)	434	448
E_0 (Mpa)	200000	200000
b	0.02	0.02

Rebar in Tension		
Parameter	#3 Rebar	#2 Rebar
σ_y (Mpa)	395	336
E_0 (Mpa)	200000	200000
b	0.0185	0.035

The calibrated analytical model formulation was implemented in Matlab and was used to compare the experimentally-observed results with analytical model predictions. The instrumentation setup established during the tests allowed local deformation measurements at various locations on the wall specimen, which were also compared with analytical model results. Analysis of the specimen RW2 was performed with the calibrated parameters defined in the previous paragraphs to validate the accuracy of the analytical model. The analyses were conducted using a displacement-controlled nonlinear analysis solution strategy. The top displacement history applied to the wall specimen included displacement components resulting from sliding and uplift of the pedestal. Hence, the analytical model was subjected to a corrected top displacement history, which was processed by subtracting the unwanted pedestal displacement effects. Analysis results were compared with the test measurements at various response levels and locations, as summarized in the next paragraphs.

Comparison of the experimentally-measured and analytically-predicted lateral load vs. top displacement response of the wall specimen is presented in Figure 5. As can be observed in the figure, the finite element model captures, with reasonable accuracy, the experimentally-observed lateral load-displacement response of the wall specimen. The analysis was conducted by applying the corrected top displacement history under a constant axial force of 378 kN. The analytically-predicted lateral load vs. displacement response reasonably represents the experimentally-observed cyclic response characteristics of the wall, including lateral load capacity, stiffness degradation, hysteretic shape,

plastic (residual) displacements, ductility, and pinching behavior. Overall, the analytical model provides an accurate prediction of the global lateral load behavior of the wall specimen.

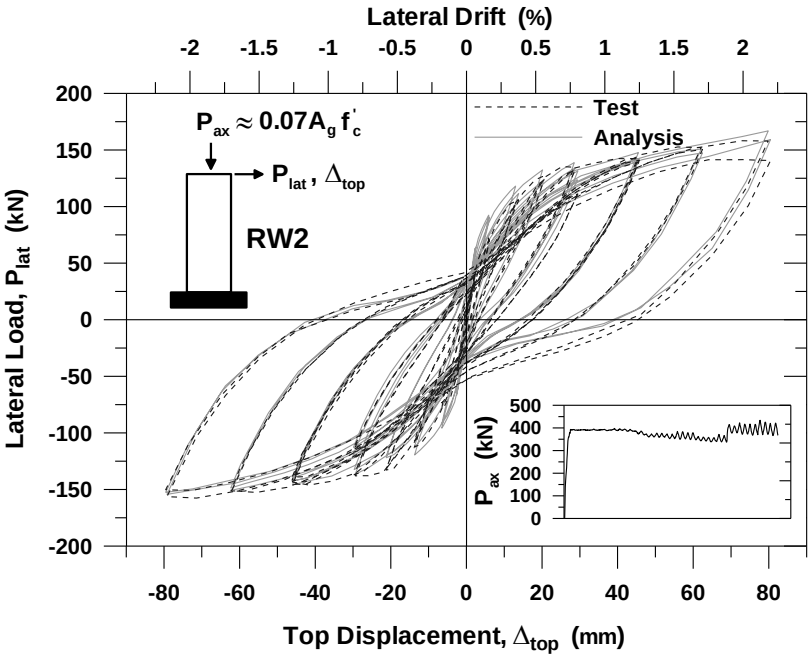

Figure 5. Comparison of the measured and calculated lateral load vs. displacement responses for wall specimen RW2.

Figure 6 presents the comparison of the experimental and analytical lateral displacement profiles of the wall, which were recorded during the test using wire potentiometers connected to the specimen at story levels (Figure 4(c)). It must be mentioned that the results compared here are the corrected lateral displacement magnitudes, meaning pedestal movement contributions were subtracted. In the positive loading direction, the model gives reasonable results at the drift levels of 1.5%, 2.0% and 2.5%, whereas in the negative direction, model predictions are more accurate at the drift levels smaller than 2.0%. Overall, the model adequately represents the distribution of lateral displacements along wall height, and concentration of nonlinear deformations along the first story height of the wall.

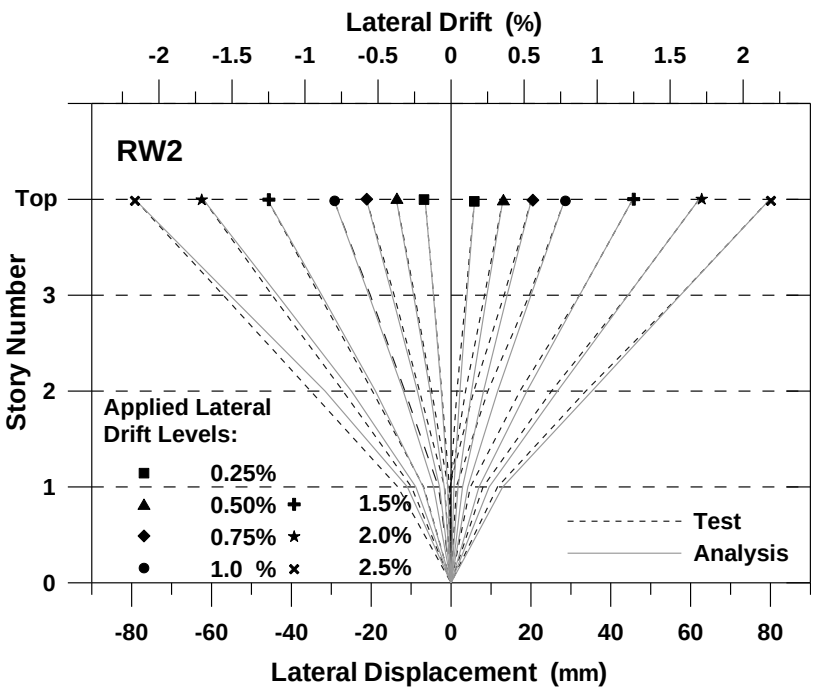

Figure 6. Comparison of the measured and predicted lateral displacement profiles.

Figure 7 compares the analytically-calculated lateral displacement and rotation time histories developing along the first story height of the wall, with the experimental measurements. In the test results, rotations over the first story were calculated by dividing the relative displacements at the end points of the wire potentiometers attached to the boundaries of the specimen by the distance between the potentiometers. The analytical predictions are sufficiently accurate to state that the analytical model reasonably predicts the nonlinear deformations developing within plastic hinge zone of the wall.

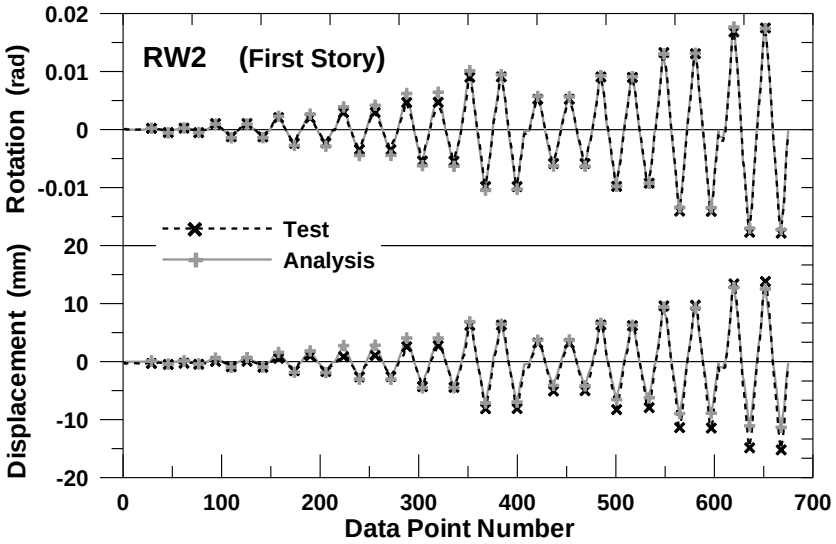

Figure 7. Comparison of measured and predicted lateral displacement and rotation time histories at the first story level.

Figure 8 compares the measured and predicted concrete strain values at specific locations and at peak points corresponding to selected drift levels. The measurements were obtained from the seven linear variable differential transducers (LVDTs) mounted at the base of the specimen (Figure 4(c)). While evaluating the analytical results, obtained vertical displacement values at model DOFs were divided by the vertical length of the model elements to calculate the average strain values. Results were compared at selected drift levels, as shown in Figure 8. As revealed in the comparisons, measured and predicted strain profiles are similar, especially in the compression region of the wall cross-section. As obviously depicted in the figure, unlike in fiber models, plane sections do not necessarily remain plane in the implemented FEM, which is more consistent with the experimentally-measured strain profiles. Accurate predictions are also obtained for the depth of the neutral axis. In the tension region of the wall cross-section, the model seems to moderately underestimate average tensile strains at large drift levels.

Figure 9 shows the comparison of the measured and predicted average strain histories in the vertical direction at the base the wall specimen. The test data was recorded by one of the LVDTs mounted at the base of the wall, located at the wall boundary. As discussed for Figure 8, the analytical model accurately captures the average compression strains in concrete, but may underestimate tensile strains at large drift levels. However, reasonable tensile strain predictions are obtained during earlier stages of loading, at smaller drift levels.

Shear distortion of the wall specimen was measured along the first and second story heights, by using diagonally-mounted wire potentiometers (Figure 4(c)). Wire potentiometers were mounted as in an X configuration along the first and second stories of the specimen. Based on measurements of these sensors and using the procedure proposed by Thomsen and Wallace (1995), shear distortions along the first and second stories of the wall were calculated and compared with the model predictions. Measured and predicted lateral load vs. shear distortion responses along the first and second story heights of the specimen are compared in Figures 10(a) and (b). In the analytical model results, significant nonlinear shear deformation response was observed along the first story, similarly to the experimental behavior; however, maximum shear deformation values were slightly underestimated

(Figure 10.(a)). It is anticipated that improving the shear aggregate interlock model in the model formulation will help capture the measured maximum shear deformation values.

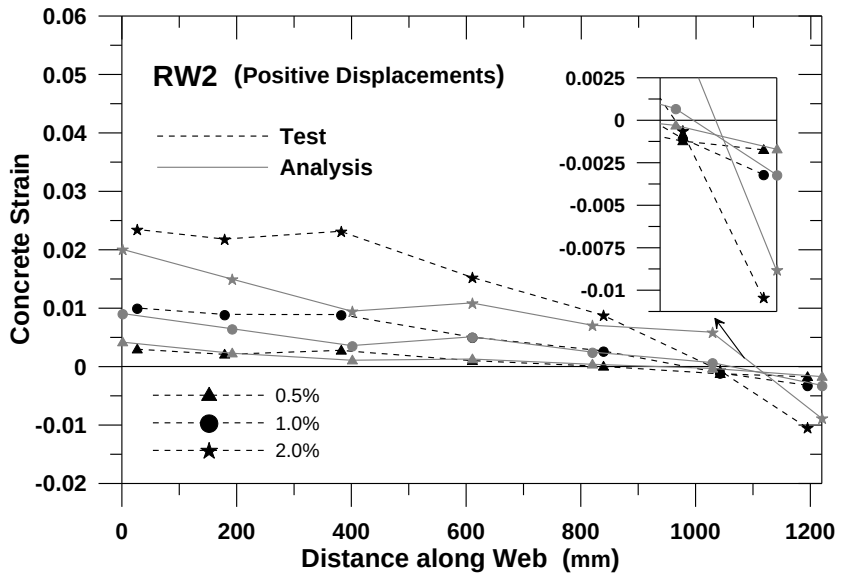

Figure 8. Comparison of the average concrete strain profiles along wall length at various drift levels.

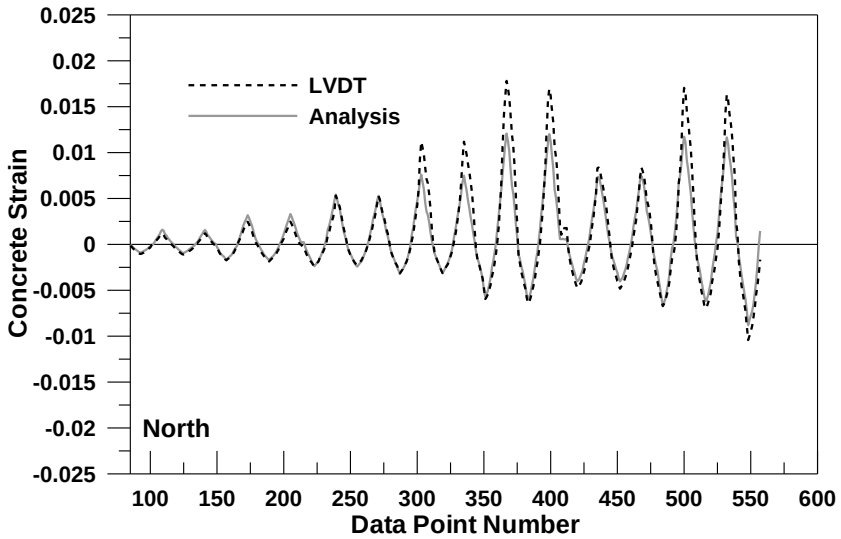

Figure 9. Comparison of the vertical strain histories at the north boundary of the wall at base level.

Figure 10(b) compares the load vs. shear deformation responses along the second story of the wall specimen. In both analytical and experimental results, the lateral load vs. shear distortion response along the second story is more linear elastic, with considerably smaller deformations compared to the first story. The analytical model reasonably captured the experimentally-observed shear deformations levels in the second story. The shear stiffness of the measured and predicted responses were not equal, but similar overall. Since shear deformations along the third and fourth stories of the wall were not experimentally measured, shear response comparisons could not be made in these regions. However, as can be observed in the results, shear deformation magnitudes decrease from the bottom story of the wall to the one above. The first story experiences the most nonlinear shear response, while the response along the second story shows less nonlinearity, and third and fourth stories would be expected to demonstrate almost linear elastic responses. Significant nonlinearity in the shear response along the first story of the wall implies that shear yielding and nonlinear shear deformations in the wall were concentrated along the plastic hinge region of the wall, where nonlinear flexural deformations are also concentrated. This demonstrates the model's capability of capturing

shear-flexure interaction effects even in a relatively slender wall, and coupling of nonlinear shear and flexural deformations throughout the cyclic loading history. This is a significant advantage of the finite element modeling approach proposed in this study, over commonly-used fiber model formulations that do not consider interaction between nonlinear flexural and shear behavior.

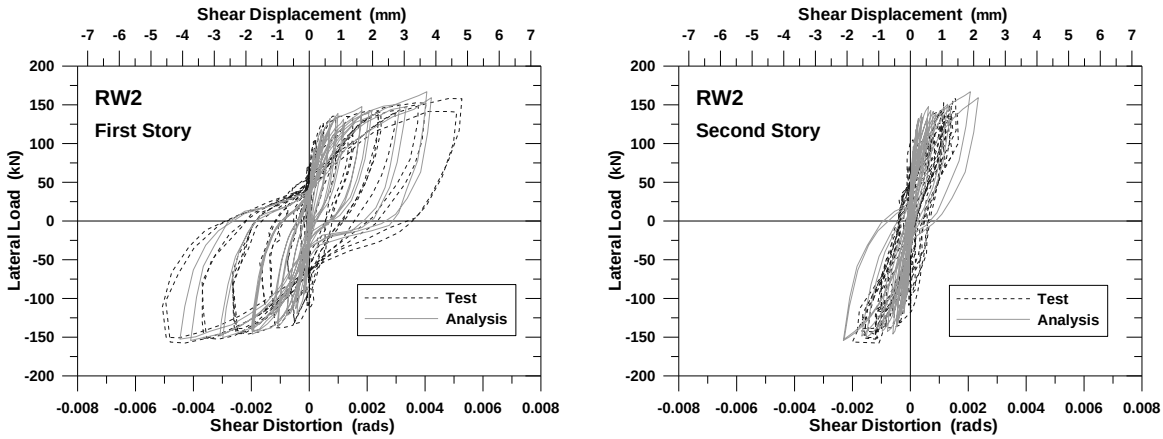

(a) (b)

Figure 10. Comparison of measured and predicted lateral load vs. shear deformation responses at: a) first story, b) second story.

CONCLUSIONS

The proposed FEM demonstrated a reasonable level accuracy in predicting the nonlinear hysteretic response of RC structural walls under in-plane reversed-cyclic loading conditions. Accurate predictions were obtained for the experimentally-observed cyclic response characteristics of the wall investigated, including its lateral load capacity, stiffness degradation, hysteretic shape, plastic (residual) displacements, ductility, and pinching behavior. The model also provided reasonably accurate predictions of nonlinear flexural deformations developing in the plastic hinge region of the wall.

Average concrete strain profiles along the base of the wall were reasonably predicted by the analytical model, especially in the compression region of the wall cross-section. Unlike in fiber models, plane sections do not necessarily remain plane in the proposed FEM formulation, which was observed to be more consistent with the experimentally-measured strain profiles. Accurate predictions were also obtained with the model for the depth of the neutral axis. Tensile strains were moderately underestimated at large drift levels.

The analytical model, with the shear aggregate interlock model formulation implemented in this study, provided reasonable estimates for the nonlinear shear deformations developing along the first story height of the wall specimen, where nonlinear flexural deformations were also concentrated. The magnitude of the predicted nonlinear shear deformations decreased along the height of the wall, which was consistent with the experimental measurements. This demonstrated the model's capability of capturing nonlinear shear-flexure interaction effects in a wall. This is a major advantage of the finite element modeling approach used in this study, over conventional fiber models that do not consider coupling of shear and flexural responses.

REFERENCES

ACI Committee 318, 2011, Building Code Requirements for Structural Concrete (ACI-318) and Commentary, American Concrete Institute, Farmington Hills, MI.

Belarbi, A. and T. C. Hsu, 1994, "Constitutive Laws of Concrete in Tension and Reinforcing Bars Stiffened By Concrete", *ACI Structural Journal*, Vol. 91, No. 4, pp. 465-474.

Chang, G. A. and J. B. Mander, 1994, Seismic Energy Based Fatigue Damage Analysis of Bridge Columns: Part I-Evaluation of Seismic Capacity, NCEER Report No. 94-0006, National Center for Earthquake Engineering Research.

Elmorsi, M., M. R. Kianush and W. K. Tso, 1998, "Nonlinear Analysis of Cyclically Loaded Reinforced Concrete Structures", *ACI Structural Journal*, Vol. 95, No. 6, pp. 725-739.

Fischinger, M, T. Vidic, J. Selih, P. Fajfar, H.Y. Zhang and F.B. Damjanic, 1990, "Validation of a Macroscopic Model for Cyclic Response Prediction of RC Walls", in N.B. Bicanic and H. Mang (eds.), *Computer Aided Analysis and Design of Concrete Structures*, Vol. 2, Pineridge Press, Swansea, pp. 1131-1142.

Gérin, M. and P. Adebar, 2009, "Simple Rational Model for Reinforced Concrete Subjected to Seismic Shear", *ASCE Journal of Structural Engineering*, Vol. 135, No. 7, pp. 753-761.

Gopalaratnman, V. S. and S. P. Shah, 1985, "Softening Response of Plain Concrete under Direct Tension", *Journal of the American Concrete Institute*, Vol. 82, No. 3, pp. 310-323.

Gullu, M. F., 2013, Finite Element Modeling Reinforced Concrete Structural Walls, MS. Thesis, Boğaziçi University.

Kolozvari, K., T. Tran, J. W. Wallace and K. Orakcal, 2012, "Modeling of Cyclic Shear-Flexure Interaction in Reinforced Concrete Structural Walls", *Proceedings*, *15th World Conference on Earthquake Engineering*, Lisbon, Portugal, No. 2471.

Mander, J. B., M. J. N Priestley and R. Park, 1988, "Theoretical Stress-Strain Model for Confined Concrete", *ASCE Journal of Structural Engineering*, Vol. 114, No. 8, pp. 1804-1826.

Mansour, M. Y., T. C. Hsu and J.Y. Lee, 2002, "Pinching Effect in Hysteretic Loops of R/C Shear Elements", *ACI Special Publications*, Vol. 205, pp. 293-321.

Matlab v.7.6.0.324 (R2008a), 2008, The Math-Works, Inc., Massachusetts USA.

Menegotto, M. and E. Pinto, 1973, "Method of Analysis for Cyclically Loaded Reinforced Concrete Plane Frames Including Changes in Geometry and Non-Elastic Behavior of Elements under Combined Normal Force and Bending", *Proceedings*, *IABSE Symposium on Resistance and Ultimate Deformability of Structures Acted on by Well-Defined Repeated Loads*, Lisbon, Portugal.

Orakcal, K., D. Ulugteking and L. M. Massone, 2012, "Constitutive Modeling of Reinforced Concrete Panel Behavior under Cyclic Loading" *Proceedings*, *15th World Conference on Earthquake Engineering*, Lisbon, Portugal, No. 3573.

Orakcal, K., J. W. Wallace and J. P. Conte, 2004, "Flexural Modeling of Reinforced Concrete Walls – Model Attributes", *ACI Structural Journal*, Vol. 101, No. 5, pp. 688-699.

Pang, D. and T. C. Hsu, 1995, "Behavior of Reinforced Concrete Membrane Elements in Shear", *ACI Structural Journal*, Vol. 92, No. 6, pp. 665-677.

Saatçioğlu, M. and S. Razvi, 1992, "Strength and Ductility of Confined Concrete", *ASCE Journal of Structural Engineering*, Vol. 118, No. 6, pp. 1590-1607.

Thomsen, J. H. and J. W. Wallace, 1995, Displacement-Based Design of Reinforced Concrete Structural Walls: An Experimental Investigation of Walls with Rectangular and T-Shaped Cross-Sections, Report No. CU/CEE-95/06, Department of Civil Engineering, Clarkson University, Postdam, New York.

Ulugtekin, D., 2010, Analytical Modeling of Reinforced Concrete Panel Elements under Reversed Cyclic Loadings, MS. Thesis, Boğaziçi University.

Vecchio, F. J. and M. P. Collins, 1986, "The Modified Compression-Field Theory for Reinforced Concrete Elements Subjected to Shear", *ACI Structural Journal*, Vol. 83, No. 2, pp. 219-231.

Vecchio, F. J. and M. P. Collins, 1993, "Compression Response of Cracked Reinforced Concrete", *ASCE Journal of Structural Engineering*, Vol. 83, No. 2, pp. 219-231.

Vulcano, A., V. V. Bertero and V. Colotti, 1988, "Analytical Modeling of RC Structural Walls", *Proceedings*, *9th World Conference on Earthquake Engineering,* Vol. 6, Tokyo-Kyoto, Japan, pp. 41-46.

Yankelevsky, D. Z. and H. W. Reinhardt, 1987, "Response of Plain Concrete to Cyclic Tension", *ACI Materials Journal*, Vol. 84, No. 5, pp. 365-373.